Reliability of Axially Compressed Cylindrical Shells With General Nonsymmetric Imperfections

Isaac Elishakoff
Professor,
Department of Aeronautical Engineering,
Technion-Israel Institute of Technology,
Haifa, Israel

Johann Arbocz
Professor of Aircraft Structures,
Department of Aerospace Engineering,
Delft University of Technology,
Delft, The Netherlands

This paper deals with the effect of general, nonsymmetric random imperfections on the reliability of axially compressed cylindrical shells. Reliability is defined here as the probability of the structure not buckling below some fixed load. The paper is a sequel to an earlier study on cylindrical shells with axisymmetric imperfections. The problem is solved by the Monte Carlo Method. The initial imperfection functions are simulated via a numerical procedure, and the buckling load of each realization of the simulated initial imperfections is found by the Multimode Analysis. It is shown that the results of existing Initial Imperfection Data Banks can be directly incorporated in the reliability analysis. Experimental information and the data derived from it, rather than theoretical assumptions, is used for constructing the reliability-based design curves for shell structures.

Introduction

It is now generally recognized that initial geometric imperfections play a dominant role in reducing the buckling load of certain structures. As is well known, an axially compressed thin shell is highly imperfection sensitive in this context (see, for example, the surveys [1-3]).

This conclusion is mainly due to the work of a series of investigators [4-6], who arrived at it through recourse to specialized imperfections. However, despite the accepted theoretical explanation of the buckling behavior of these structures, the use of the concept of imperfection sensitivity in engineering practice is still in the ad-hoc stage and engineers prefer to rely on the "knockdown factor" [7] chosen so that its product with the classical buckling load yields a lower bound to available experimental data for the configuration in question. This apparent reluctance to take advantage of theoretical findings stems from the fact that most imperfection studies are conditional on detailed advance knowledge of the geometric imperfections of the particular structure, which is rarely possible. In an ideal case the imperfections can be measured experimentally and incorporated in the theoretical analysis to predict the buckling loads. This approach, however, while justified for single prototype-like structures, is impracticable as a general method of behavior prediction. Information on the type and magnitude of imperfections of a particular structure would be too specific and are not strictly valid for other realizations of the same structure even those obtained by the same manufacturing process.

In the light of these considerations and bearing in mind the scatter of the experimental results, it appears obvious that practical applications of the imperfection-sensitivity theories are conditional on their being combined with a statistical analysis of the imperfections and critical loads. The notion of randomness of the initial imperfections was given considerable attention in the literature, and a bibliography can be found in Amazigo's paper [8]. For the single-mode solutions the reader should consult Bolotin [9] (who pioneered the probabilistic approach to buckling) and Roorda [10].

Recently, Elishakoff [11-13] suggested to utilize the Monte Carlo Method for the solution of multimode problems involving random initial imperfection sensitivity. This method represents a logical remedy in view of the difficulties inherent in purely analytical approaches (based on unnecessary and often very restrictive assumptions on the properties of the initial imperfections and/or using heavily simplified solution procedures).

The first step of the Monte Carlo Method consists of simulating the random initial imperfection profiles via a special numerical procedure [14]; the second step comprises a numerical solution of the buckling problem for every realization of the initial imperfection profile; the third and last step involves a statistical analysis of the buckling loads (for a detailed description of the Monte Carlo Method see reference [15]). The reliability is determined as the fraction of an ensemble of shells of which the buckling loads exceed the specified load. In a recent paper the present writers [16] have applied the Monte Carlo Method to shells with random axisymmetric imperfections. In this paper, the same method will be applied to general nonsymmetric random imperfections.

To the best of our knowledge, there are three works that

Contributed by the Applied Mechanics Division for publication in the JOURNAL OF APPLIED MECHANICS.

Discussion on this paper should be addressed to the Editorial Department, ASME, United Engineering Center, 345 East 47th Street, New York, N. Y. 10017, and will be accepted until two months after final publication of the paper itself in the JOURNAL OF APPLIED MECHANICS. Manuscript received by ASME Applied Mechanics Division, April, 1982; final revision, November, 1983.

Downloaded From: https://appliedmechanics.asmedigitalcollection.asme.org on 06/29/2019 Terms of Use: http://www.asme.org/about-asme/terms-of-use
Copyright © 1985 by ASME

have been devoted to the analysis of cylindrical shells with general nonsymmetric random imperfections. Makaroff [17], at the Moscow Energetics Institute, carried out systematic analysis of initial imperfections. He used series of 30 cylindrical shells made of sheets of electrical grade pressboard. The initial imperfection was represented as a double Fourier series and the coefficients were treated as random variables. The analysis showed that the assumption of circumferential homogeneity of the initial imperfections was satisfactory (within the confidence limits used in the analysis), and the normality of their Fourier coefficients did not conflict with the experimental data. Makaroff also carried out a theoretical analysis of the buckling of stochastically imperfect shells, with the experimental data obtained earlier serving as the input for the description of the imperfections. He found a theoretical mean buckling load that exceeds its experimental counterpart by a factor of 1.35.

Fersht [18] generalized the method of truncated hierarchy, used earlier by Amazigo [19] for axisymmetric random imperfections, to include the nonsymmetric case. It turned out that for nonsymmetric imperfections a closed-form expression for the buckling load is unattainable and rather cumbersome numerical integrations have to be performed. Moreover, for the axisymmetric case, Fersht's numerical results do not agree with those of Amazigo [19].

Hansen [20] generalized his previous deterministic results of reference [21]. The main conclusion was that the imperfection parameters associated with the nonaxisymmetric modes appear only in three separate summations and the behavior of the system is governed by the values of these summations rather than by the individual imperfection amplitudes. It was assumed that the Fourier coefficients of the initial imperfections are jointly normal random variables with zero mean, that they are statistically independent and are identically distributed. Then the Monte Carlo Method was applied. For each sample problem the buckling load was found via the method of reference [21] and then the mean buckling loads were calculated. The role of the nonaxisymmetric imperfections turned out to be very important.

Probabilistic Properties and Simulation of the Initial Imperfections for a Finite Shell

Let us represent the initial imperfection functions as the following series

$$W_0(\xi,\theta)=\sum_{i=0}^{N_1} A_i\cos\, i\pi\xi+\sum_{k=1}^{N_2}\sum_{l=1}^{N_3}(C_{kl}\sin k\pi\xi\,\cos\, l\theta + D_{kl}\,\sin\, k\pi\xi\,\sin\, l\theta) \tag{1}$$

where

$$W_0(\xi,\theta)=\frac{w_0(\xi,\theta)}{t},\quad \xi=\frac{x}{L},\quad \theta=\frac{y}{R},\quad 0\le x\le L,\quad 0\le\theta\le 2\pi$$

$w_0(\xi,\theta)$ and $W_0(\xi,\theta)$ are dimensional and nondimensional initial imperfections; t, L, and R are the thickness, the length, and the radius of the shell, respectively; x is the axial and y is the circumferential coordinate. Notice that in equation (1) the first sum represents the axisymmetric part of the initial imperfection profile, whereas the second, double sum is associated with its nonsymmetric part. The axisymmetric part is expressed in the half-range cosine series, whereas the nonsymmetric part is represented by the half-range sine series, so that the series (1) sums up to the measured imperfection profile in the range $0\le x\le L$, $0\le\theta\le 2\pi$.

The mathematical expectation of $W_0(\xi,\theta)$ is given by

$$\langle W_0(\xi,\theta)\rangle=\sum_{i=0}^{N_1}\langle A_i\rangle\cos\, i\pi\xi+\sum_{k=1}^{N_2}\sum_{l=1}^{N_3}(\langle C_{kl}\rangle\sin\, k\pi\xi\,\cos\, l\theta + \langle D_{kl}\rangle\sin\, k\pi\xi\,\sin\, l\theta) \tag{2}$$

where $\langle\ \ldots\ \rangle$ denotes a mathematical expectation.

The autocovariance function becomes

$$\begin{aligned}C_{W_0}(\xi_1,\theta_1;\xi_2,\theta_2)&=\langle[W_0(\xi_1,\theta_1)-\langle W_0(\xi_1,\theta_1)\rangle][W_0(\xi_2,\theta_2)-\langle W_0(\xi_2,\theta_2)\rangle]\rangle\\&=\Big\langle\Big[\sum_{i=0}^{N_1}(A_i-\langle A_i\rangle)\cos\, i\pi\xi_1+\sum_{k=1}^{N_2}\sum_{l=1}^{N_3}(C_{kl}-\langle C_{kl}\rangle)\sin\, k\pi\xi_1\,\cos\, l\theta_1+\sum_{k=1}^{N_2}\sum_{l=1}^{N_3}(D_{kl}-\langle D_{kl}\rangle)\sin\, k\pi\xi_1\,\sin\, l\theta_1\Big]\\&\times\Big[\sum_{j=0}^{N_1}(A_j-\langle A_j\rangle)\cos\, j\pi\xi_2+\sum_{m=1}^{N_2}\sum_{n=1}^{N_3}(C_{mn}-\langle C_{mn}\rangle)\sin\, m\pi\xi_2\,\cos\, n\theta_2+\sum_{m=1}^{N_2}\sum_{n=1}^{N_3}(D_{mn}-\langle D_{mn}\rangle)\sin\, m\pi\xi_2\,\sin\, n\theta_2\Big]\Big\rangle\end{aligned} \tag{3}$$

For the sake of simplicity we rewrite equation (1) in an alternative way, replacing the double summation in equation (1) by a single summation

$$W_0(\xi,\theta)=\sum_{i=1}^{N_1}A_i\cos\, i\pi\xi+\sum_{r=1}^{N}(C_r\,\sin\, k_r\pi\xi\,\cos\, l_r\theta + D_r\,\sin\, k_r\pi\xi\,\sin\, l_r\theta) \tag{4}$$

where the quantities indexed with r are chosen so as to ensure the equivalence of the two series given by equations (1) and (4) and $N=N_2\times N_3$. The autocovariance function can be written as

$$\begin{aligned}C_{W_0}(\xi_1,\theta_1;\xi_2,\theta_2)&=\sum_{i=0}^{N_1}\sum_{j=0}^{N_1}K_{A_iA_j}\cos\, i\pi\xi_1\,\cos\, j\pi\xi_2+\sum_{i=0}^{N_1}\sum_{s=1}^{N}K_{A_iC_s}\cos\, i\pi\xi_1\,\sin\, k_s\pi\xi_2\,\cos\, l_s\theta_2+\sum_{i=0}^{N_1}\sum_{s=0}^{N}K_{A_iD_s}\cos\, i\pi\xi_1\,\sin\, k_s\pi\xi_2\,\sin\, l_s\theta_2\\&+\sum_{r=1}^{N}\sum_{j=0}^{N_1}K_{C_rA_j}\sin\, k_r\pi\xi_1\,\cos\, l_r\theta_1\,\cos\, j\pi\xi_2+\sum_{r=1}^{N}\sum_{j=0}^{N_1}K_{D_rA_j}\sin\, k_r\pi\xi_1\,\sin\, l_r\theta_1\,\cos\, j\pi\xi_2\\&+\sum_{r=1}^{N}\sum_{s=1}^{N}K_{C_rC_s}\sin\, k_r\pi\xi_1\,\cos\, l_r\theta_1\,\sin\, k_s\pi\xi_2\,\cos\, l_s\theta_2+\sum_{r=1}^{N}\sum_{s=1}^{N}K_{C_rD_s}\sin\, k_r\pi\xi_1\,\cos\, l_r\theta_1\,\sin\, k_s\pi\xi_2\,\sin\, l_s\theta_2\end{aligned} \tag{5}$$

Downloaded From: https://appliedmechanics.asmedigitalcollection.asme.org on 06/29/2019 Terms of Use: http://www.asme.org/about-asme/terms-of-use

$$+\sum_{r=1}^{N}\sum_{s=1}^{N} K_{D_rC_s} \sin k_r\pi\xi_1 \sin l_r\theta_1 \sin k_s\pi\xi_2 \cos l_s\theta_2$$

$$+\sum_{r=1}^{N}\sum_{s=1}^{N} K_{D_rD_s} \sin k_r\pi\xi_1 \sin l_r\theta_1 \sin k_s\pi\xi_2 \sin l_s\theta_2$$

where the variance-covariance matrices $K_{A_iA_j}$, . . . , etc. are defined as follows:

$$\begin{aligned}
K_{A_iA_j} &= \langle (A_i - \langle A_i \rangle)(A_j - \langle A_j \rangle) \rangle \\
K_{A_iC_s} &= \langle (A_i - \langle A_i \rangle)(C_s - \langle C_s \rangle) \rangle \\
K_{A_iD_s} &= \langle (A_i - \langle A_i \rangle)(D_s - \langle D_s \rangle) \rangle \\
K_{C_rC_s} &= \langle (C_r - \langle C_r \rangle)(C_s - \langle C_s \rangle) \rangle \\
K_{C_rD_s} &= \langle (C_r - \langle C_r \rangle)(D_s - \langle D_s \rangle) \rangle \\
K_{D_rD_s} &= \langle (D_r - \langle D_r \rangle)(D_s - \langle D_s \rangle) \rangle
\end{aligned} \tag{6}$$

If the autocovariance function $C_{W_0}(\xi_1, \theta_1; \xi_2, \theta_2)$ is known, then these quantities can be obtained as follows:

$$K_{A_iA_j} = \frac{1}{\pi^2}\int_0^{2\pi}\int_0^1\int_0^{2\pi}\int_0^1 C_{W_0}(\xi_1,\theta_1;\xi_2,\theta_2)$$

$$\times \cos i\pi\xi_1 \cos j\pi\xi_2 d\xi_1 d\theta_1 d\xi_2 d\theta_2$$

$$K_{A_iC_{mn}} = \frac{2}{\pi^2}\int_0^{2\pi}\int_0^1\int_0^{2\pi}\int_0^1 C_{W_0}(\xi_1,\theta_1;\xi_2,\theta_2)$$

$$\times \cos i\pi\xi_1 \sin m\pi\xi_2 \cos n\theta_2 \, d\xi_1 \, d\theta_1 \, d\xi_2 \, d\theta_2$$

$$K_{A_iD_{mn}} = \frac{2}{\pi^2}\int_0^{2\pi}\int_0^1\int_0^{2\pi}\int_0^1 C_{W_0}(\xi_1,\theta_1;\xi_2,\theta_2)$$

$$\times \cos i\pi\xi_1 \sin m\pi\xi_2 \sin n\theta_2 \, d\xi_1 \, d\theta_1 \, d\xi_2 \, d\theta_2$$

$$K_{A_jC_{kl}} = \frac{2}{\pi^2}\int_0^{2\pi}\int_0^1\int_0^{2\pi}\int_0^1 C_{W_0}(\xi_1,\theta_1;\xi_2,\theta_2)$$

$$\times \cos j\pi\xi_2 \sin k\pi\xi_1 \cos l\theta_1 \, d\xi_1 \, d\theta_1 \, d\xi_2 \, d\theta_2$$

$$K_{A_jC_{kl}} = \frac{2}{\pi^2}\int_0^{2\pi}\int_0^1\int_0^{2\pi}\int_0^1 C_{W_0}(\xi_1,\theta_1;\xi_2,\theta_2)$$

$$\times \cos j\pi\xi_2 \sin k\pi\xi_1 \sin l\theta_1 \, d\xi_1 \, d\theta_1 \, d\xi_2 \, d\theta_2$$

$$K_{C_{kl}C_{mn}} = \frac{4}{\pi^2}\int_0^{2\pi}\int_0^1\int_0^{2\pi}\int_0^1 C_{W_0}(\xi_1,\theta_1;\xi_2,\theta_2)$$

$$\times \sin k\pi\xi_1 \cos l\theta_1 \sin m\pi\xi_2 \cos n\theta_2 \, d\xi_1 \, d\theta_1 \, d\xi_2 \, d\theta_2$$

$$K_{D_{kl}C_{mn}} = \frac{4}{\pi^2}\int_0^{2\pi}\int_0^1\int_0^{2\pi}\int_0^1 C_{W_0}(\xi_1,\theta_1;\xi_2,\theta_2)$$

$$\times \sin k\pi\xi_1 \sin l\theta_1 \sin m\pi\xi_2 \cos n\theta_2 \, d\xi_1 \, d\theta_1 \, d\xi_2 \, d\theta_2$$

$$K_{D_{kl}D_{mn}} = \frac{4}{\pi^2}\int_0^{2\pi}\int_0^1\int_0^{2\pi}\int_0^1 C_{W_0}(\xi_1,\theta_1;\xi_2,\theta_2)$$

$$\sin k\pi\xi_1 \sin l\theta_1 \sin m\pi\xi_2 \sin n\theta_2 \, d\xi_1 \, d\theta_1 \, d\xi_2 \, d\theta_2 \tag{7}$$

Notice that if $W_0(\xi,\theta)$ is constant and

$$K_{A_iC_s} = K_{A_iD_s} = K_{C_rA_j} = K_{D_rA_j} = K_{C_rD_s} = K_{D_rC_s} = 0 \tag{8}$$

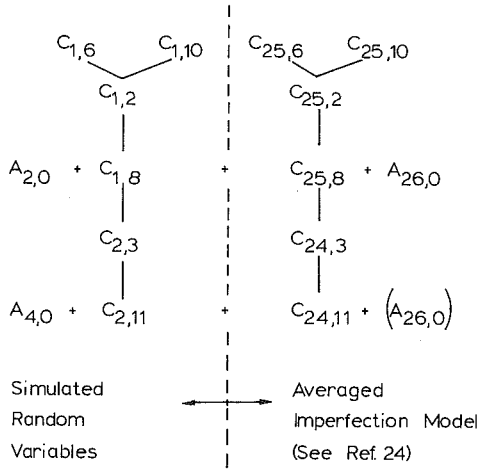

Fig. 1 Modified 15 modes imperfection model used for Monte Carlo method

for any combination of indices, and moreover

$$\begin{aligned}
K_{C_rC_s} &= K_{D_rD_s} \\
K_{C_rC_s} &= K_{C_rC_r}\delta_{l_rl_s}
\end{aligned} \tag{9}$$

where $\delta_{l_rl_s}$ is a Kronecker delta, then the initial imperfection is a weakly homogeneous function in the circumferential direction. Under the conditions (8) and (9) the autocovariance function takes the form

$$C_{W_0}(\xi_1,\theta_1;\xi_2,\theta_2) = \sum_{i=0}^{N_1}\sum_{j=0}^{N_1} K_{A_iA_j} \cos i\pi\xi_1 \cos j\pi\xi_2$$

$$+\sum_{r=1}^{N}\sum_{s=1}^{N} K_{C_rC_s} \sin k_r\pi\xi_1 \sin k_s\pi\xi_2 \cos l_r(\theta_2 - \theta_1) \tag{10}$$

i.e., it depends on $\theta_2 - \theta_1$ rather than on θ_1 and θ_2 separately. It can be shown that equations (8) and (9) represent not only the sufficient conditions but also the necessary ones. One could argue, that for the closed, nominally circular, seamless cylindrical shell the probabilistic properties would not be affected by a shift of the origin of the coordinate axes in the circumferential direction. Interestingly, in Makaroff's experiments [17] this weak homogeneity was preserved even for the series of shells with pronounced seams. Due to the frequent use of this property we will first show how to simulate the initial imperfections possessing weak homogeneity in the circumferential direction.

To simulate the large number of initial imperfection profiles needed for the Monte Carlo Method, first the mean values and the variance-covariance matrices of the measured initial imperfections must be determined. This involves the evaluation of the following ensemble averages for a sample of experimentally measured initial imperfections:

$$\tilde{A}_i^{(e)} = \frac{1}{M}\sum_{m=1}^{M} A_i^{(m)}; \quad \tilde{C}_r^{(e)} = \frac{1}{M}\sum_{m=1}^{M} C_r^{(m)}$$

$$K_{A_iA_j}^{(e)} = \frac{1}{M-1}\sum_{m=1}^{M} [A_i^{(m)} - \tilde{A}_i^{(e)}][A_j^{(m)} - \tilde{A}_j^{(e)}]$$

$$K_{C_rC_s}^{(e)} = \frac{1}{M-1}\sum_{m=1}^{M} [C_r^{(m)} - \tilde{C}_r^{(e)}][C_s^{(m)} - \tilde{C}_s^{(e)}] \tag{11}$$

where M is the number of sample shells, and m is the serial number of the shells. The variance-covariance matrices are positive-semidefinite and can be uniquely decomposed in the form

$$[K_{A_iA_j}^{(e)}] = [G][G]^T, [K_{C_rC_s}^{(e)}] = [G'][G']^T \tag{12}$$

Downloaded From: https://appliedmechanics.asmedigitalcollection.asme.org on 06/29/2019 Terms of Use: http://www.asme.org/about-asme/terms-of-use

where T means transpose and $[G]$, $[G']$ are lower-triangular matrices found by the Cholesky decomposition algorithm. Now we form the random vectors $\{B\}$ and $\{B'\}$, the elements of which are normally distributed, statistically independent with zero means and unit variance. Then the vectors of the Fourier coefficients of the initial imperfections are simulated as follows:

$$\{A\} = [G]\{B\} + \{\tilde{A}^{(e)}\}, \quad \{C\} = [G']\{B'\} + \{\tilde{C}^{(e)}\} \quad (13)$$

Having the desired large number of realizations of the vectors $\{B\}$ and $\{B'\}$ one obtains the same number of realizations of $\{A\}$ and $\{C\}$. The mean feature of this simulation technique [14] is that it is applicable for homogeneous, as well as nonhomogeneous random functions with given mean and autocovariance functions.

Equation (13) represents the simulated vectors $\{A\}$ and $\{C\}$ for the random imperfections, weakly homogeneous in the circumferential direction. For the imperfections which form a general nonhomogeneous random field, the refined simulation procedure, developed in reference [22] has to be utilized. The essence of this refinement is the replacement of the multiple summations in equations (2) and (4) by a single "string" and the dealing with the resultant mixed series (for details see reference [22]).

Multimode Deterministic Analysis for Each Realization of Random Initial Imperfections

The buckling load for each created shell is then calculated by the so-called Multimode analysis [23], which allows the incorporation of imperfection shapes in the form of the double Fourier series given in equation (1). By definition, the value of the loading parameter λ corresponding to the limit point of the prebuckling states is the theoretical buckling load. The number of modes of deformation included in the analysis is limited by practical considerations, like the available core size and the time required for obtaining the solution. Thus, since the shell buckling load will be determined by solving the governing equations for a particular set of modes, an attempt of optimizing the selection of these modes must be made. That is, it is necessary to locate those modes that dominate the prebuckling and buckling behavior of the shell. Previous investigations by Arbocz and Babcock [23, 24] have shown that to yield a noticeable decrease from the buckling load of the perfect shell, the initial imperfection harmonics used must include at least one mode with a significant initial amplitude and an associated eigenvalue that is close to the buckling load of the perfect shell. Furthermore, if the modes are so selected that the nonlinear coupling conditions are satisfied then the resulting buckling load of the shell generally will be lower than the buckling loads obtained with each mode considered separately.

Based on these considerations and the results published in reference [24] the imperfection model shown in Fig. 1 was selected for the Monte Carlo simulation. In this model $A_{2,0}$ stands for a half-wave cosine axisymmetric Fourier coefficient, with two half-waves in the axial direction and no waves in the circumferential direction. On the other hand $C_{1,10}$ stands for an asymmetric Fourier coefficient with a single half-wave in the axial direction and 10 full waves in the circumferential direction.

As pointed out in reference [24] the chosen imperfection model requires imperfection amplitudes at wave numbers that were not measured. This is due to the fact that in the early experimental work the mesh-spacing used was not sufficiently close to resolve all the harmonic amplitudes of interest. Therefore the Donnell-Imbert [25] imperfection model was fitted over the wave numbers actually measured and then the amplitudes of the harmonics of interest were obtained by extrapolation. It should be stressed here that the averaged (in

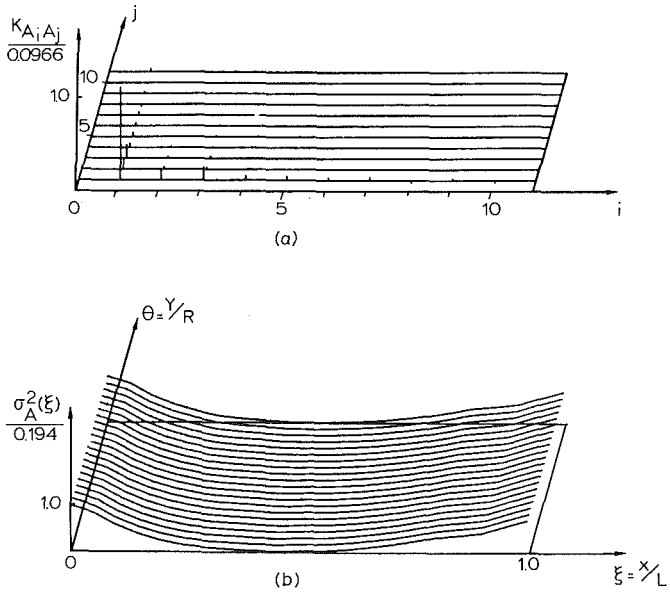

Fig. 2 *(a)* **Elements of cross-correlation matrix $K_{A_iA_j}$ for simulated group of 500 *B*-shells, and *(b)* corresponding part of variance**

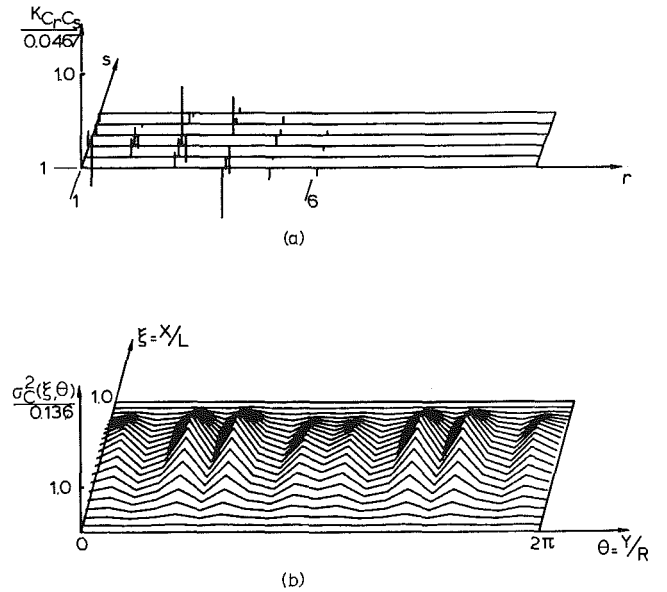

Fig. 3 *(a)* **Elements of cross-correlation matrix $K_{C_rC_s}$ for simulated group of 500 *B*-shells, and *(b)* corresponding part of variance**

the axial direction short wavelength) modes of the imperfection model shown in Fig. 1 must be included in the analysis in order to satisfy the nonlinear coupling conditions. Their initial amplitudes are actually insignificant.

For the purpose of the Monte Carlo Method the MIUTAM code [24] was incorporated into a new program, which then one by one automatically starts the calculations for the simulated imperfections and at the end lists all the buckling loads obtained.

Numerical Results and Discussion

The procedure described in the previous sections was applied to the group of shells, referred in reference [26] as *B*-shells. These shells were originally cut from thickwalled seamless brass tubing; the pieces were mounted on a mandrel and the outer surface was machined to the desired dimen-

Downloaded From: https://appliedmechanics.asmedigitalcollection.asme.org on 06/29/2019 Terms of Use: http://www.asme.org/about-asme/terms-of-use

Table 1 Fourier coefficients of *B*-shells

Coefficients \ Shell	*B*-1	*B*-2	*B*-3	*B*-4	Mean values
$A_{2,0}$	−0.0108	−0.0272	−0.0899	−0.0176	−0.0364
$A_{4,0}$	0.0226	−0.0078	−0.0255	−0.0096	−0.0050
$C_{1,2}$	0.417	0.393	0.741	0.223	0.4435
$C_{1,6}$	−0.078	−0.143	0.017	0.078	−0.0315
$C_{1,8}$	−0.264	−0.009	0.112	0.102	−0.0148
$C_{1,10}$	0.037	0.044	−0.246	−0.009	−0.0435
$C_{2,3}$	−0.101	0.034	−0.065	−0.002	−0.0335
$C_{2,11}$	0.010	−0.009	−0.028	0.014	−0.0033
$D_{1,2}$	0.024	−0.203	0.147	0.029	−0.0008
$D_{1,6}$	−0.390	0.058	0.128	−0.248	−0.1130
$D_{1,8}$	−0.029	0.087	0.185	−0.050	0.0483
$D_{1,10}$	−0.013	0.039	−0.031	−0.051	−0.0140
$D_{2,3}$	−0.070	−0.047	0.040	−0.015	−0.0230
$D_{2,11}$	0.013	−0.018	−0.004	0.002	−0.0018

For the group of *B*-shells:
$R = 101.6$ mm, $t = 0.2050$ mm, $L = 196.85$ mm,
$E = 1.065 \times 10^5$ N/mm^2, $\nu = 0.3$.
Note: Here $w_0^{(m)}$ is positive outward.

Table 2 Variance-covariance matrices $K_{C_rC_s}$ and $K_{D_rD_s}$

$K_{C_rC_s} =$

1,2	1,6	1,8	1,10	2,3	2,11	
0.46861^{-1}	-0.87197^{-3}	0.61544^{-2}	-0.24776^{-1}	-0.59778^{-2}	-0.37388^{-2}	1,2
-0.87197^{-3}	0.96697^{-2}	0.99562^{-2}	-0.65293^{-2}	-0.83271^{-3}	0.20500^{-3}	1,6
0.61544^{-2}	0.99562^{-2}	0.30567^{-1}	-0.13717^{-1}	0.56447^{-2}	-0.14967^{-2}	1,8
-0.24776^{-1}	-0.65293^{-2}	-0.13717^{-1}	0.18684^{-1}	0.26231^{-2}	0.20676^{-2}	1,10
-0.59778^{-2}	-0.83271^{-3}	0.56447^{-2}	0.26231^{-2}	0.37104^{-2}	0.21989^{-4}	2,3
-0.37388^{-2}	0.20500^{-3}	-0.14967^{-2}	0.20676^{-2}	0.21989^{-4}	0.36852^{-3}	2,11

$K_{D_rD_s} =$

1,2	1,6	1,8	1,10	2,3	2,11	
0.21394^{-1}	-0.33159^{-2}	0.24798^{-2}	-0.47927^{-2}	0.43517^{-2}	0.11773^{-2}	1,2
-0.33159^{-2}	0.60673^{-1}	0.24746^{-1}	0.32506^{-2}	0.76675^{-2}	-0.26069^{-2}	1,6
0.24798^{-2}	0.24746^{-1}	0.11956^{-1}	0.11053^{-2}	0.35032^{-2}	-0.80206^{-3}	1,8
-0.47927^{-2}	0.32506^{-2}	0.11053^{-2}	0.14992^{-2}	-0.88147^{-3}	-0.32594^{-3}	1,10
0.43517^{-2}	0.76675^{-2}	0.35032^{-2}	-0.88147^{-3}	0.22434^{-2}	-0.12750^{-3}	2,3
0.11773^{-2}	-0.26069^{-2}	-0.80206^{-3}	-0.32594^{-3}	-0.12750^{-3}	0.16719^{-3}	2,11

sions. The geometric and material properties of the *B*-shells are summarized in Table 1.

As is seen from Fig. 1, the simulation procedure was applied only to the eight lower order modes, namely $A_{2,0}$, $A_{4,0}$, $C_{1,2}$, $C_{1,6}$, $C_{1,8}$, $C_{1,10}$, $C_{2,3}$, and $C_{2,11}$. The remaining seven higher-order modes, namely $A_{26,0}$, $C_{24,3}$, $C_{24,11}$, $C_{25,2}$, and $C_{25,10}$ were obtained by extrapolation from the corresponding Donnell-Imbert imperfection model [24, 25].

Figure 2 shows the elements of the variance-covariance matrices $K_{A_iA_j}$ and the corresponding part of the variance, denoted by $\sigma^2{}_A(\xi)$

$$\sigma^2{}_A(\xi) = \sum_{i=0}^{N_1} \sum_{j=0} K_{A_iA_j}\, \delta_{ij} \cos\pi i\xi \cos\pi j\xi \tag{15}$$

For fixed ξ, this part of the variance is constant, since equation (15) is associated with the axisymmetric part of the imperfections.

Figures 3 and 4 show the elements of the variance-covariance matrices $K_{C_rC_s}$ and $K_{D_rD_s}$, respectively, and the associated parts of the variance, denoted by $\sigma^2{}_C(\xi,\theta)$ and $\sigma^2{}_D(\xi,\theta)$:

$$\sigma^2{}_C(\xi,\theta) = \sum_{r=1}^{N} \sum_{s=1}^{N} K_{C_rC_s} \times \sin k_r\pi\xi \sin k_s\pi\xi \cos l_r\theta \cos l_s\theta \tag{16}$$

$$\sigma^2{}_D(\xi,\theta) = \sum_{r=1}^{N} \sum_{s=1}^{N} K_{D_rD_s} \times \sin k_r\pi\xi \sin k_s\pi\xi \sin l_r\theta \sin l_s\theta \tag{17}$$

Figure 5 portrays the probabilistic characteristics of the 500 simulated shells. Figure 5(*a*) shows the mean imperfection function, whereas Fig. 5(*b*) displays the variance. As is seen from Fig. 5 neither the mean function nor the variance are constant in the circumferential direction, implying that the random imperfections do not constitute a circumferentially homogeneous field. This conclusion can also be deduced from Table 2, which lists the values of $K_{C_rC_s}$ and $K_{D_rD_s}$. An examination of this table reveals that the corresponding elements of these matrices not only do not coincide, but a

Downloaded From: https://appliedmechanics.asmedigitalcollection.asme.org on 06/29/2019 Terms of Use: http://www.asme.org/about-asme/terms-of-use

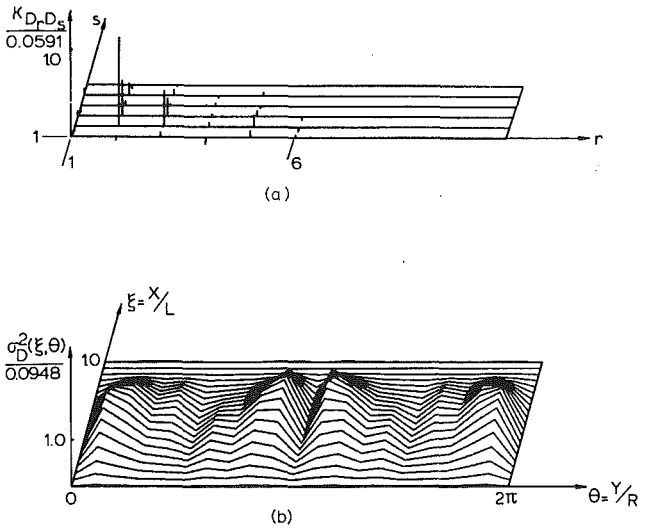

Fig. 4 (a) Elements of cross-correlation matrix $K_{D_r D_s}$ for simulated group of 500 *B*-shells, and (*b*) corresponding part of variance

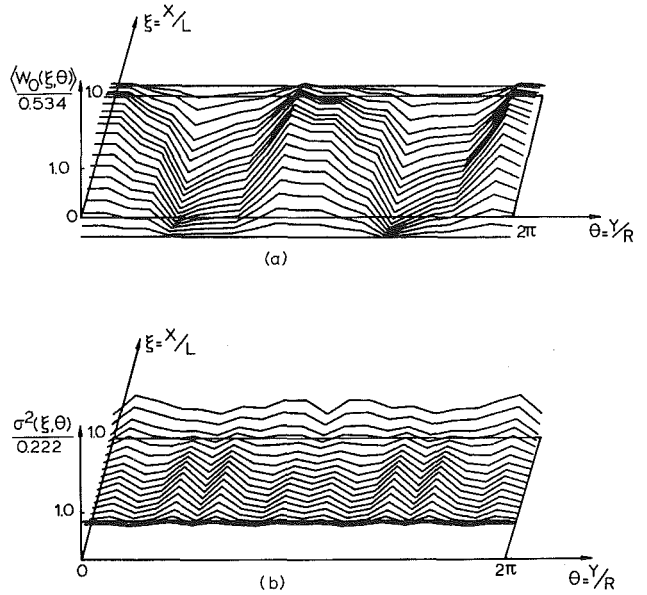

Fig. 5 Probabilistic characteristics of the simulated group of 500 *B*-shells. (*a*) mean function, and (*b*) variance.

ratio between them may well exceed 10. Thus the homogeneity assumption adopted in reference [8] turns out to be unjustifiable even for seamless shells.

To calculate the reliability functions shown in Fig. 6 the following dimensions corresponding to shell *B*-1 [26] were used: length of 196.85 mm, radius of 101.60 mm, and thickness of 0.205 mm. In addition, for the buckling load calculations of shells with axisymmetric imperfections the one-sided transfer-function shown in Fig. 7 was chosen. This was done due to the fact [27], that for a finite length shell the buckling load is sensitive only to those axisymmetric imperfections that point inward at the mid-plane of the shell (at $x = L/2$).

In Fig. 6, curve 1 represents the reliability function for the case of purely axisymmetric imperfections (with an estimated mean buckling load of 0.935), whereas curve 2 shows the reliability function for the 15-modes nonsymmetric imperfection mode (with an estimated mean buckling load of 0.739). As can be seen, the reliability estimate depends strongly on the number of terms taken into account, i.e., it is

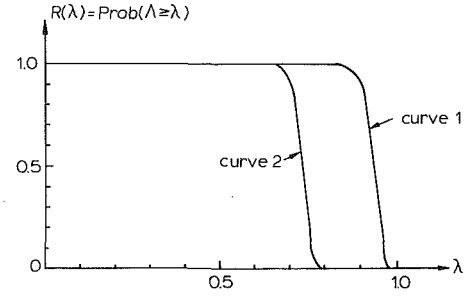

Fig. 6 Reliability functions for simulated group of 500 *B*-shells

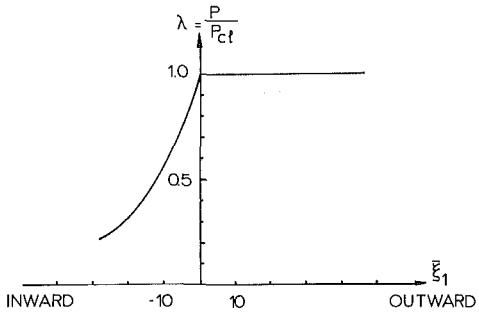

Fig. 7 One-sided transfer function used for axisymmetric imperfections only [27]

sensitive to the adequacy of the underlying deterministic model. As a check on the correctness of the simulated results the 15-modes imperfection model shown in Fig. 1 was used to calculate the collapse loads of the original four *B*-shells involved, using the experimentally measured initial imperfections in place of the simulated random variables. These computations yielded for the shells *B*-1, *B*-2, *B*-3, and *B*-4, respectively, the following collapse loads 0.751, 0.746, 0.740, and 0.781 with a mean of 0.756. Closeness to the simulated results is remarkable. It should also be mentioned here that the theoretical collapse load of $\rho_s = 0.66$, reported in reference [24] for the shell *B*-1, was entirely based on the Donnell-Imbert [25] imperfection model. Considering the results shown in Fig. 6 further, one sees that the inclusion of some asymmetric imperfection components has reduced the estimate of the mean buckling load considerably, though it is still higher than the experimental mean buckling load for the group of B-shells of 0.592 [26]. However, as work currently in progress has shown, further refinements in the nonsymmetric random imperfection model will lead to lower simulated buckling loads.

Conclusions

One can summarize the results obtained so far as follows:

1 It has been demonstrated that the Monte Carlo Method can be used successfully to obtain reliability functions for shells with axisymmetric as well as asymmetric imperfections.

2 It has been found that for finite shells, nonstationary statistic must be used (thus ergodicity is strictly speaking not applicable).

3 Using the simulation procedure developed by Elishakoff [11, 22] the measured initial imperfections have been used directly to generate input for the Monte Carlo Method.

It is hoped that these preliminary results will encourage many investigators all over the world to compile extensive

Downloaded From: https://appliedmechanics.asmedigitalcollection.asme.org on 06/29/2019 Terms of Use: http://www.asme.org/about-asme/terms-of-use

experimental information on initial imperfections classified according to the manufacturing procedures. The existence of these Initial Imperfection Data Banks will make it possible to associate statistical measures with the different methods of fabrication. As outlined in this paper, the variance-covariance matrices and the mean vectors can be used effectively to generate input for the Monte Carlo Method, which in turn yields the reliability functions associated with the different manufacturing processes. It is felt that by this means the imperfection sensitivity concept can be finally introduced routinely into the design procedures since the Monte Carlo Method described in this paper seems to offer the means of combining the Lower Bound Design Philosophy with the notion of Goodness Classes. Thus shells manufactured by a process, which produces inherently a less damaging initial imperfection distribution, will not be penalized because of the low experimental results obtained with shells produced by another process, which generates a more damaging characteristic initial imperfection distribution.

Acknowledgment

This work has been supported by the Delft University of Technology during I. Elishakoff's sabbatical stay at the Department of Aerospace Engineering in 1979/1980 and by the Dutch Foundation of the Technical Sciences (STW) during a visit in the summer of 1983. These aids and the warm and kind hospitality are gratefully acknowledged. Thanks are also due to the Technion Research Promotion Fund for partial support of this study.

References

1 Hutchinson, J. W., and Koiter, W. T., "Postbuckling Theory," ASME *Applied Mechanics Review*, Dec. 1970, pp. 1353–1366.

2 Tvergaard, V., "Buckling Behaviour of Plate and Shell Structure," in *Theoretical and Applied Mechanics*, Koiter, W. T., ed., North-Holland, 1976, pp. 233–247.

3 Budiansky, B., and Hutchinson, J. W., "Buckling: Progress and Challenge," in *Trends in Solid Mechanics 1979*, Proceedings of the Symposium Dedicated to the 65th Birthday of W. T. Koiter, Besseling, J. F., and Van der Heijden, A. M. A., eds., Sijthoff and Nordhoff, Alphen aan den Rijn, 1979, pp. 93–116.

4 Donnell, L. H., and Wan, C. C., "Effect of Imperfections on the Buckling of Thin Cylinders and Columns Under Axial Compression," ASME JOURNAL OF APPLIED MECHANICS, Vol. 17, 1950, pp. 73–83.

5 Koiter, W. T., "The Effect of Axisymmetric Imperfections on the Buckling of Cylindrical Shells Under Axial Compression," *Proceedings of the Royal Netherlands Academy of Sciences*, Amsterdam, Series B., Vol. 66, No. 5, 1963, pp. 265–279.

6 Budiansky, B., and Hutchinson, J. W., "Dynamic Buckling of Imperfection Sensitive Structures," in *Proceedings of the Eleventh Congress on Theoretical and Applied Mechanics*, Gortler, M., ed., Springer-Verlag, Berlin, 1964, pp. 636–651.

7 NASA, "Buckling of Thin-Walled Circular Cylinders," NASA SP 8007, Aug. 1968.

8 Amazigo, J. C., "Buckling of Stochastically Imperfect Structures," in *Buckling of Structures*, Budiansky, B., ed., IUTAM Symposium, Cambridge, Mass., 1974, Springer-Verlag, Berlin, 1976, pp. 172–182.

9 Bolotin, V. V., *Statistical Methods in Structural Mechanics*, Holden-Day, San Francisco, 1969.

10 Roorda, J., *Buckling of Elastic Structures*, University of Waterloo Press, 1980.

11 Elishakoff, I., "Impact Buckling of Thin Bar Via Monte Carlo Method," ASME JOURNAL OF APPLIED MECHANICS, Vol. 45, 1978, pp. 586–590.

12 Elishakoff, I., "Buckling of a Stochastically Imperfect Finite Column on a Nonlinear Elastic Foundation—A Reliability Study," ASME JOURNAL OF APPLIED MECHANICS, Vol. 46, 1979, pp. 411–416.

13 Elishakoff, I., "Hoff's Problem in a Probabilistic Setting," ASME JOURNAL OF APPLIED MECHANICS, Vol. 47, 1980, pp. 403–408.

14 Elishakoff, I., "Simulation of Space-Random Fields for Solution of Stochastic Boundary-Value Problems," *Journal of the Acoustical Society of America*, Vol. 65, No. 2, 1979, pp. 399–403.

15 Elishakoff, I., *Probabilistic Methods in the Theory of Structures*, Wiley-Interscience, New York, 1983, pp. 433–468.

16 Elishakoff, I., and Arbocz, J., "Reliability of Axially Compressed Cylindrical Shells With Random Axisymmetric Imperfections," *International Journal of Solids and Structures*, Vol. 18, 1982, pp. 563–585.

17 Makaroff, B. P., "Statistical Analysis of Deformation of Imperfect Cylindrical Shells," in *Strength Calculations* (in Russian), Vol. 15, 1971, Moscow "Mashinostroenie" Publishing House, pp. 240–256.

18 Fersht, R., "Buckling of Cylindrical Shells With Random Imperfections," in *Thin Shell Structures, Theory, Experiment and Design*, Fung, Y. C., and Sechler, E. E., eds., Prentice-Hall, Englewood Cliffs, N.J., 1974, pp. 325–341.

19 Amazigo, J. C., "Buckling Under Axial Compression of Long Cylindrical Shells with Random Axisymmetric Imperfections," *Quarterly of Applied Mathematics*, Vol. 26, 1969, pp. 537–566.

20 Hansen, J., "General Random Imperfections in the Buckling of Axially Loaded Cylindrical Shells," *AIAA Journal*, Vol. 15, 1977, pp. 1250–1256.

21 Hansen, J., "Influence of General Imperfections in Axially Loaded Cylindrical Shells," *International Journal of Solids and Structures*, Vol. 11, 1975, pp. 1223–1233.

22 Elishakoff, I., "Simulation of an Initial Imperfection Data Bank, Part 1: Isotropic Shells With General Imperfections," TAE Report 500, Department of Aeronautical Engineering, Technion-Israel Institute of Technology, Haifa, Israel, July, 1982.

23 Arbocz, J., and Babcock, C. D., Jr., "A Multi-Mode Analysis for Calculating Buckling Loads of Imperfect Cylindrical Shells," GALCIT Report SM-74-4, California Institute of Technology, Pasadena, Calif., June 1974.

24 Arbocz, J., and Babcock, C. D., "Prediction of Buckling Loads Based on Experimentally Measured Initial Imperfections" in *Buckling of Structures*, Budiansky, B., ed., IUTAM Symposium, Cambridge, Mass., 1974, Springer-Verlag, Berlin, 1976, pp. 291–311.

25 Imbert, K., "The Effect of Imperfections on the Buckling of Cylindrical Shells," Aeronautical Engineer Thesis, California Institute of Technology, Pasadena, Calif., June 1971.

26 Arbocz, J., and Abramovich, H., "The Initial Imperfection Data Bank at the Delft University of Technology—Part I," Report LR-290, Department of Aerospace Engineering, Delft University of Technology, Delft, The Netherlands, Dec., 1979.

27 Babcock, C. D., Jr., and Sechler, E. E., "The Effect of Initial Imperfections on the Buckling Stress of Cylindrical Shells," NASA TN D-1510, Dec. 1962, pp. 135–142.

Downloaded From: https://appliedmechanics.asmedigitalcollection.asme.org on 06/29/2019 Terms of Use: http://www.asme.org/about-asme/terms-of-use